Molecular Neurobiology (2024) 61:6675–6687
https://doi.org/10.1007/s12035-024-03956-5

Contribution of ApoB-100/SORT1-Mediated Immune Microenvironment in Regulating Oxidative Stress, Inflammation, and Ferroptosis After Spinal Cord Injury

Chunshuai Wu[1,2,3] · Chunyan Ji[1,2,3] · Dandan Qian[1,2,3] · Chaochen Li[1,2,3] · Jiajia Chen[1] · Jinlong Zhang[1] · Guofeng Bao[1,2,3] · Guanhua Xu[1,2,3] · Zhiming Cui[1,2,3]

Received: 30 October 2023 / Accepted: 12 January 2024 / Published online: 10 February 2024

Abstract

This study aims to explore the impacts of ApoB-100/SORT1-mediated immune microenvironment during acute spinal cord injury (SCI), and to investigate the potential mechanism. CB57BL/6 mice underwent moderate thoracic contusion injury to establish the SCI animal model, and received ApoB-100 lentivirus injection to interfere ApoB-100 level. Functional recovery was assessed using the Basso, Beattie, and Bresnahan (BBB) score and footprint analysis. Transmission electron microscopy was applied to observe the ultrastructure of the injured spinal cord tissue. Hematoxylin-eosin (HE) staining and Perls staining were conducted to assess histological changes and iron deposition. Biochemical factor and cytokines were detected using their commercial kits. M1/M2 macrophage markers were detected by immunofluorescence assay in vivo and by flow cytometry in vitro. HT22 neurons were simulated by lipopolysaccharide (LPS), followed by incubation with polarized macrophage medium to simulate the immune microenvironment of injured spinal cord in vitro. The local immune microenvironment is changed in SCI mice, accompanied with the occurrence of oxidative stress and the elevation of both M1 and M2 macrophages. Knockdown of ApoB-100 ameliorates oxidative stress and lipid disorder, and inhibits inflammation and ferroptosis in SCI mice. Importantly, knockdown of ApoB-100 can partly restrict M1 macrophages but does not change M2 macrophage proportion in SCI mice. Further, M1 macrophages are observed to attenuate the inflammatory response, oxidative stress, and ferroptosis levels of LPS-induced HT22 cells, which is further strengthened by SORT1 knockdown. Blockage of ApoB-100/SORT1-mediated immune microenvironment plays a protective role against SCI via inhibiting oxidative stress, inflammation, lipid disorders, and ferroptosis, providing novel insights of the targeted therapy of SCI.

Keywords Acute spinal cord injury · Macrophages · ApoB-100 · SORT1

Introduction

Traumatic central nervous system (CNS) injuries include traumatic brain injury and spinal cord injury (SCI) [1]. SCI can be divided into primary injuries caused by the direct action of mechanical external forces on the injured area leading to the damage of nerves, blood vessels, and other parenchymal tissues (also called acute SCI), and secondary injuries caused by a series of cascade reactions caused by changes in the local microenvironment leading to secondary nerve damage [2]. SCI affects 2 to 3 million people worldwide, increasing by 250,000 to 500,000 annually [3]. The total lifetime costs for patients suffering from SCI exceed 3 million dollars, causing a major economic burden worldwide [4]. Further, the high rate of disability and mortality of SCI is devastating [5, 6].

Chunshuai Wu and Chunyan Ji contributed equally to this work.

✉ Guanhua Xu
guanhua_xu@163.com

✉ Zhiming Cui
Cuizhim831022@163.com

[1] Department of Spinal Surgery, The Second Affiliated Hospital of Nantong University, Nantong First People's Hospital, Nantong University, 666 Shengli Road, Nantong 226000, Jiangsu Province, China

[2] Research Institute for Spine and Spinal Cord Disease of Nantong University, Nantong 226000, China

[3] Key Laboratory for Restoration Mechanism and Clinical Translation of Spinal Cord Injury, Nantong 226000, China

A previous study has shown that the number of immune cells such as lymphocytes and macrophages in the acute stage of SCI is relatively high, thus presenting distinct polarization phenotypes and activity levels under the influence of inducible factors in different environments. In addition, when SCI occurs, macrophages in the injured area are the first to be attacked, where M1-type macrophages and M2-type macrophages are increased, but M1-type macrophages are more significant [7]. Recent studies are more inclined to improve SCI immune microenvironment and repair tissue damage by inducing differentiation of M2-type macrophage cells with anti-inflammatory activities [8]. However, in fact, M1-type cells with proinflammatory activity also partly contribute to tissue repair in SCI. M1-type macrophages themselves express high level of Ly6C and secrete proinflammatory cytokines IL-1β and TNF-α to exert strong phagocytosis and proteolytic functions. Moreover, M1-type macrophages can activate adaptive immunity to produce antigen presentation and activate antioxidant system, thus secreting more antioxidant enzymes such as superoxide dismutase (SOD) and glutathione (GSH). These effects are particularly important in the early stage of SCI [9]. Therefore, adjusting M1/M2 ratio according to the characteristics following SCI may have a better prospect for alleviating SCI and promoting functional recovery.

It has been reported that the level of oxidized low-density lipoprotein (ox-LDL) of SCI patients without exercise is significantly higher than that of normal population or SCI patients with regular rehabilitation exercise, and is also negatively related to the functional recovery, suggesting that a higher ox-LDL level is associated with poorer prognosis [10, 11]. Apolipoprotein B-100 (ApoB-100) is one of the major components involved in the formation of LDL complex, and LDL is particularly easy to oxidize to form ox-LDL, especially under the inflammatory condition, indicating that ApoB-100 may be an upstream factor regulating the rise of ox-LDL in non-exercise rehabilitation SCI patients [12]. Sortilin1 (SORT1), a type I transmembrane multiligand receptor, is a member of the receptor family in the Vacuolar protein sorting 10 protein (Vps10p) domain. SORT1 is widely distributed in microglia and acts as the membrane receptor of ApoB-100. The combined SORT1 and ApoB-100 can promote the transport, differentiation, and degradation of LDL, and the overexpression of SORT1 can induce the activation of the inflammatory response pathway of microglia [13, 14]. In addition, ox-LDL promotes macrophage polarization towards M1 phenotype and is closely related to inflammation and ferroptosis [15]. Therefore, it is reasonable to speculate that ApoB-100/SORT1 is critical for the formation of ox-LDL, and may be involved in ox-LDL-related pathological mechanism of SCI.

Therefore, based on the above background, we have the reason to believe that macrophages are activated after acute stage of SCI, and the seriously abnormal ratio of M1/M2 courses may be an important factor leading to poor prognosis of SCI patients. ApoB-100/SORT1-mediated abnormal LDL metabolism, lipid peroxidation, ferroptosis, macrophage polarization, and subsequently amplified inflammatory response may be the important mechanism behind the poor prognosis of acute stage of SCI.

Materials and Methods

Animals and SCI Modeling

Eight-week-old female CB57BL/6 mice (weight 27–30 g) were acquired from Cavens Biogle (Suzhou) Model Animal Research Co. Ltd. and housed under a 12-h light/dark cycle at room temperature with free access to water and food. All animal experiments in this study were approved by Nantong First People's Hospital.

Mice were randomly divided into SHAM, SCI, SHAM + ApoB-100 knockdown (KD), and SCI + ApoB-100 KD groups ($n = 6$). After the mice were anesthetized via intraperitoneal injection with 70 mg/kg ketamine and 5 mg/kg xylazine, laminectomy was performed to expose the spinal cord at T10. Thereafter, a model of SCI model was established using the modified Allen method with an impact force of 20 g × 30 mm. Lower limb convulsion and localized hematoma of the injured spinal cord in mice indicated successful modeling. After injury, the muscle layers and skin were sutured. During SCI procedure, mice were placed on a constant heating pad to maintain temperature at 37 °C. Mice in the sham group received a laminectomy, but no SCI. Mice in the SCI + ApoB-100 KD group were injected with 10 µL of lentivirus vectors carrying short hairpin RNA against ApoB-100 (5.0×10^8 TU/mL) in spinal cord tissue via a microsyringe immediately following SCI. On the 7th day after the operation, mice were euthanized, and the spinal cord tissues and blood samples were collected.

Basso, Beattie, and Bresnahan (BBB) Score

The BBB score was performed to test locomotor function of mice after SCI, which comprises 21 different criteria for the movement of lower limbs, from complete paralysis to complete mobility. These criteria are based on the accurate observation of the lower limbs, including movement, step, and coordinated motor action. The scores were recorded by two well-trained investigators who were blinded to the experiments [16].

Footprint Analysis

A narrow runway 50 cm long and 4–5 cm wide was formed by covering on the white paper. The mice were stained with red ink on the front feet and blue ink on the back feet, and then placed on the runway and allowed to walk freely. After the footprints were dried, the vertical distance between the palms of the two back feet was measured. The motor function was evaluated according to the distance.

Biochemical Analysis

Total cholesterol (TC), triglyceride (TG), high-density lipoprotein cholesterol (HDL-c), low-density lipoprotein cholesterin (LDL-c), and very-low-density lipoprotein (VLDL-p) in the peripheral blood were measured according to the instructions of the assay kits from Nanjing Jiancheng Bioengineering Institute.

Measurement of Oxidative Stress–Related Factors

The levels of SOD, malonaldehyde (MDA), GSH, and catalase (CAT) in the peripheral blood were quantified using the corresponding assay kit (Nanjing Jiancheng Bioengineering Institute, China) according to the manufacturer's instructions. In addition, to detect the level of reactive oxygen species (ROS), part of the spinal cord tissue was washed with ice-cold PBS, embedded in optimum cutting temperature compound (OCT), and then cut into slices. The frozen spinal cord slices were stained with dihydroethidium (DHE; Sigma-Aldrich) for 30 min away from the light. The images were observed under a confocal microscope.

Transmission Electron Microscopy (TEM)

The spinal cord samples were fixed with 2.5% glutaraldehyde and 1% osmium tetroxide in 0.2 mol/L sodium phosphate buffer for 12 h. After dewatering and embedding slicing, the slices were cut into 1-mm-thick sections and stained using uranyl acetate and lead citrate. The images were obtained using TEM with a JEM-1400 electron microscope (JEOL Ltd., Akishima, Tokyo, Japan) to observe subcellular structural changes of neuronal cells.

Hematoxylin–Eosin (HE) Staining and Perls Staining

The spinal cord samples were fixed with 4% paraformaldehyde at room temperature for 24 h, and then embedded in paraffin and sliced into 4-μm-thickness sections. Afterwards, these sections were stained with HE staining and Perls staining, respectively. Images were observed under a light microscope.

Immunofluorescence Staining

After deparaffinization and rehydration, the sections were subjected to heat-induced antigen retrieval in a citrate buffer for 10 min, and incubated with 3% hydrogen peroxide for 10 min to inhibit endogenous peroxidase activity. After blocking with 5% bovine serum albumin for 1 h, the sections were incubated with M1 marker antibodies CD86 and iNOS and M2 marker antibodies Arg-1 and CD206 at 4 °C overnight, followed by incubation with appropriate fluorescently labeled secondary antibody for 1 h at room temperature. Finally, the sections were stained with 4′,6-diamidino-2-phenylindole (DAPI) (Beyotime, China), and the images were observed under a confocal microscope.

Western Blot

Total protein was extracted with RIPA buffer (Beyotime, China), and subsequently, a BCA assay (Thermo Fisher Scientific, USA) was used to detect the protein concentration. A total of 30 μg of proteins was separated by SDS–polyacrylamide gel electrophoresis, which was then transferred to nitrocellulose membranes. Membranes were incubated with 5% skim milk to block reactions for 1 h. Membranes were incubated with primary antibodies overnight at 4 °C, followed by incubation with goat anti-rabbit HRP-conjugated secondary antibody at room temperature for 1 h. Bands were visualized using an enhanced chemiluminescence (ECL) reagent (Thermo Fisher Scientific), and the density of protein bands was semi-quantified using ImageJ (National Institutes of Health, Bethesda, MD, USA).

Real-Time Quantitative PCR (RT-qPCR)

Total RNA was exacted with TRIzol reagent (Invitrogen, Carlsbad, CA), and subsequently reverse-transcribed into cDNA following the manufacturer's instructions of Prime Script II 1st Strand cDNA Synthesis Kit (Takara, Dalian, China). Thereafter, real-time PCR was carried out adopting SYBR Premix Ex Taq (Takara) with a Step One Plus Real-Time PCR Detection System (Applied Biosystems, USA). Relative expression of target mRNAs was calculated with $2^{-\Delta\Delta Ct}$ method and normalized to GAPDH.

Cell Culture

Mouse mononuclear macrophage RAW 264.7 cells (CL-0190; Procell, Wuhan, China) and mouse neuron HT22 cells (CL-0697; Procell) were maintained in Dulbecco's Modified Eagle Medium (DMEM) supplemented with 10% fetal bovine serum

(FBS, Gibco, Carlsbad, CA) and 1% penicillin/streptomycin (Invitrogen, Carlsbad, CA) in a 5% CO_2 incubator at 37 °C. To induce spinal cord neuron damage model in vitro, HT22 neurons were stimulated with 0.1 g/L of lipopolysaccharide (LPS; Sigma-Aldrich) for 24 h.

Cell Transfection

Small interference RNAs targeting SORT1, including si-SORT1-1 (5′- GCAGCCTTCATATCCATGCTT-3′), si-SORT1-2 (5′-CCGTCCTATCAATGTGATTAA-3′), and si-SORT1-3 (5′-GCACCTGACAACAAATGGGTA-3′), and the negative control (si-NC) were obtained from Heyuan Biotechnology Co., Ltd. (Shanghai, China). HT22 cells were transfected with above plasmids using Lipofectamine® 3000 reagent (Invitrogen; Thermo Fisher Scientific, Inc.) following the manufacturer's protocol. After 48 h of transfection, RT-qPCR was used to detect the transfection efficiency.

Macrophage Polarization

Mouse macrophage RAW264.7 cells were treated with 20 ng/mL of IFN-γ (Sigma-Aldrich) and 100 ng/mL of LPS for 24 h to differentiate into M1 macrophages. The polarization transition was evaluated with flow cytometry analysis using PE-conjugated anti-CD206 and APC-conjugated anti-CD11c antibodies by flow cytometry (BD Biosciences, San Diego, CA, USA). Thereafter, the conditioned medium from M1 macrophages was harvested and then added to HT22 cells for further analysis.

Measurement of Inflammatory Cytokines

The supernatant levels of tumor necrosis factor-α (TNF-α), interleukin (IL-6), and IL-1β in cell culture medium were measured using quantitative enzyme-linked immunosorbent assay (ELISA) kits (Nanjing Jiancheng Bioengineering Institute, China) according to the manufacturer's instructions.

Statistics

Data are expressed as mean ± SD. Student's *t*-test was used for comparisons between two groups. For multiple comparisons, the data were analyzed by one-way ANOVA followed by Tukey post hoc tests. $p < 0.05$ was considered statistically significant.

Results

The Local Immune Microenvironment Is Changed in SCI Mice

The front feet of mice were painted red and the back feet were painted blue. Footprint analysis showed that the movement of mice in the SHAM group had nothing abnormal. The SCI group could only see red marks while no blue marks (Fig. 1A). BBB scores of mice in the SHAM group were 21 points, while those in the SCI group were 2.3 points averagely (Fig. 1B). The results indicated that mice in the SCI group had hind limb paralysis. Biochemical methods were used to detect the levels of lipid factors in peripheral blood samples of mice. The results showed that the levels of TC and VLDL-p in the SCI group were significantly increased compared with those in the SHAM group. The expression of TG and LDL also increased, but there was no significantly statistical difference, and HDL-C level was significantly decreased (Fig. 1C). The results indicated that lipid metabolism was disturbed after SCI. Subsequently, we also measured the levels of oxidative stress–related factors in peripheral blood. The results showed that compared with the SHAM group, SOD, CAT, and GSH activities were significantly decreased while MDA content was significantly increased in the SCI group (Fig. 1D), confirming the occurrence of oxidative stress following SCI, which was further validated by the increased ROS production after SCI (Fig. 1E).

In addition, immunofluorescence staining assay was conducted to assess macrophage polarization in injured spinal cord tissues following SCI. Compared with the SHAM group, the CD206-positive and Arg-1-positive cells were markedly elevated in the SCI group. Meanwhile, the CD86-positive and iNOS-positive cells were slightly elevated in the SCI group compared to those in the SHAM group. Moreover, it was found that in the SCI group, the proportion and distribution of M2 macrophages were superior to M1 macrophages (Fig. 2). These findings suggested that both M1 and M2 macrophages were elevated following SCI, and M2 macrophages were dominant.

Knockdown of ApoB-100 Improves Oxidative Stress and Lipid Metabolism in SCI Mice

The mice were divided into SHAM, SCI, SHAM + ApoB-100 KD, and SCI + ApoB-100 KD groups. Combined with the results of the BBB score and footprint analysis, mice in each group exhibited normal motor function before surgery. On day 7 after surgery, both the BBB score and vertical distance between the two hind feet of mice were decreased in the SCI group compared with those of the SHAM group. It was worth noting that, compared with the SCI group, ApoB-100 knockdown effectively improved the BBB functional score and also slightly prolonged vertical distance between the two hind feet of mice (Fig. 3A, B), suggesting that ApoB-100 knockdown could improve functional recovery of locomotion of SCI mice.

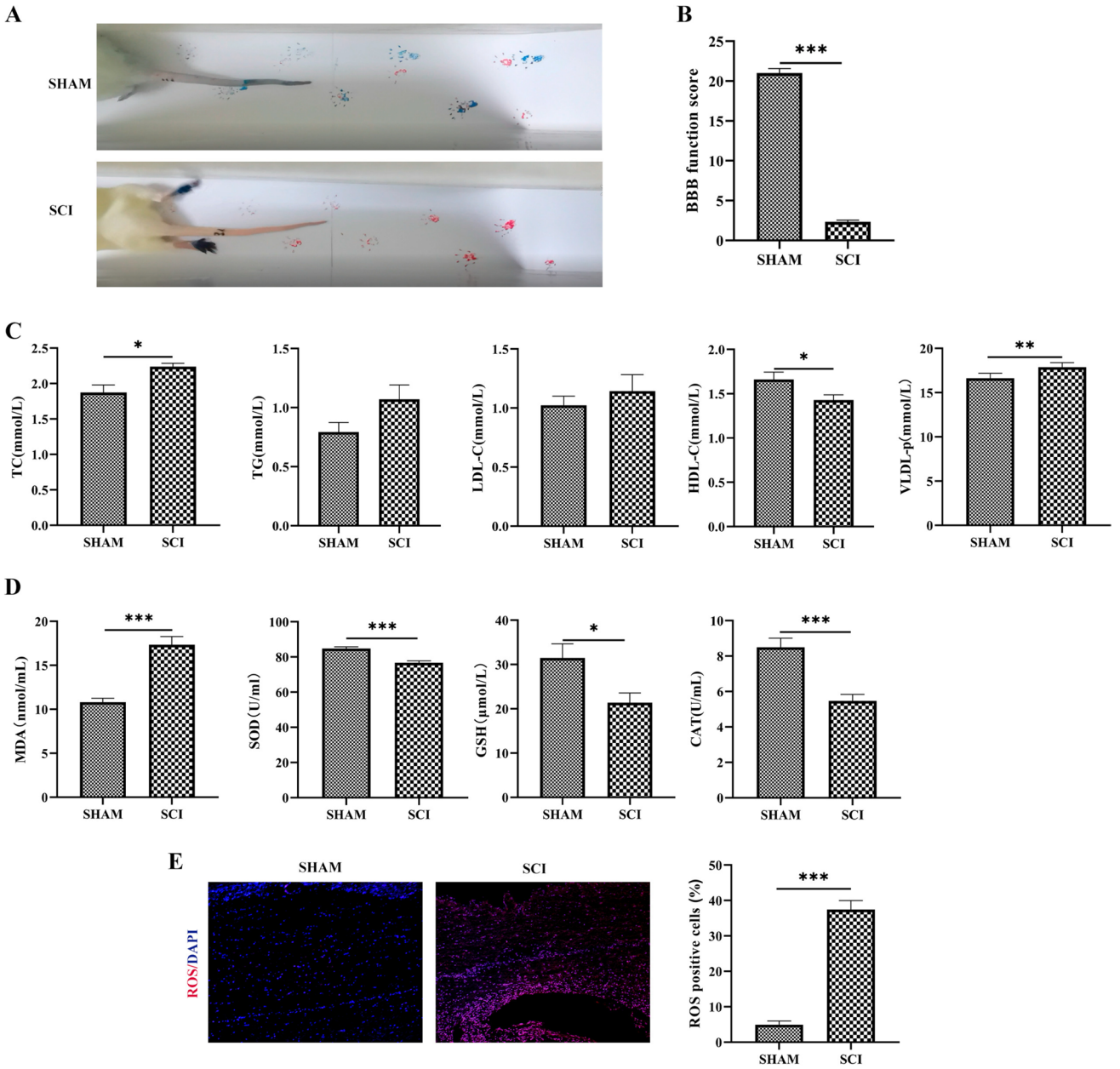

Fig. 1 The changes of functional recovery, lipid factors, and oxidative stress following SCI in mice. **A** Footprints were used to detect the movement of mice. **B** BBB score was used to test motor function of mice. **C** Biochemical methods were used to detect the levels of lipid factors in peripheral blood samples of mice. **D** The kits were used to measure the levels of oxidative stress–related factors in peripheral blood. **E** Representative images of ROS staining of spinal cord tissues. $^{*}p < 0.05$, $^{**}p < 0.01$, and $^{***}p < 0.001$

The results of biochemical analysis showed that compared with the SHAM group, the activities of SOD, GSH, and CAT in the SCI group were significantly decreased, while ApoB-100 knockdown partly inhibited improved SOD and CAT activities (Fig. 4A). Meanwhile, the elevated ROS level following SCI was significantly reduced by ApoB-100 knockdown (Fig. 4B), confirming that ApoB-100 knockdown could inhibit oxidative stress in SCI mice. In addition, as exhibited in Fig. 4C, the levels of lipid metabolism–related factors including TC, TG, and LDL-c were increased while the level of HDL-c was decreased in the SCI group compared with those in the SHAM group. Compared with the SCI group, the levels of TC, TG, and LDL-c in the SCI + ApoB-100 KD group were decreased, suggesting that ApoB-100 knockdown could partly restore the dysregulation of lipid metabolism following SCI.

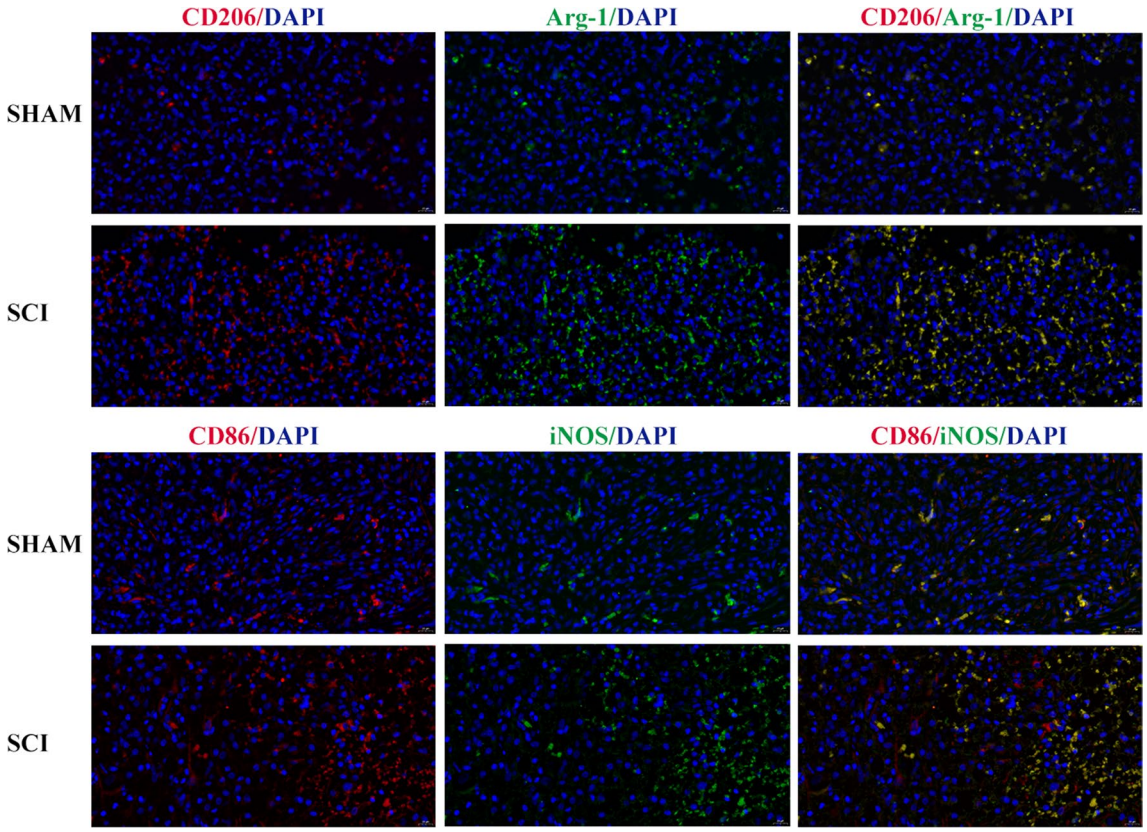

Fig. 2 Representative images of immunofluorescence staining of M1/M2 macrophage markers in spinal cord tissues

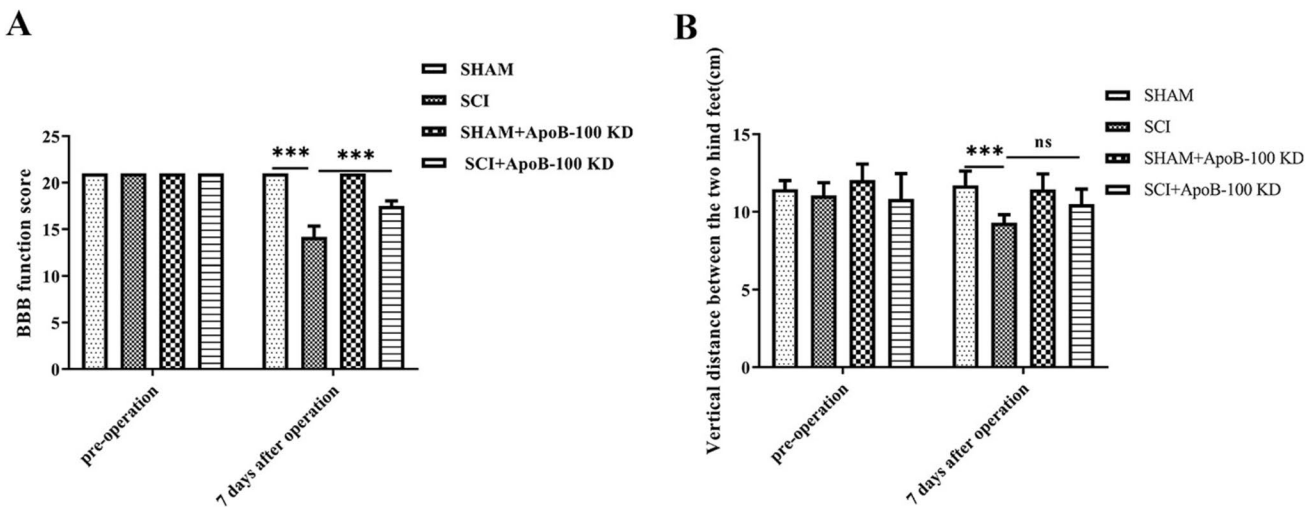

Fig. 3 Knockdown of ApoB-100 improves functional recovery of SCI mice. **A** BBB score was used to test motor function of mice. **B** Footprints were used to detect the movement of mice. ***$p < 0.001$

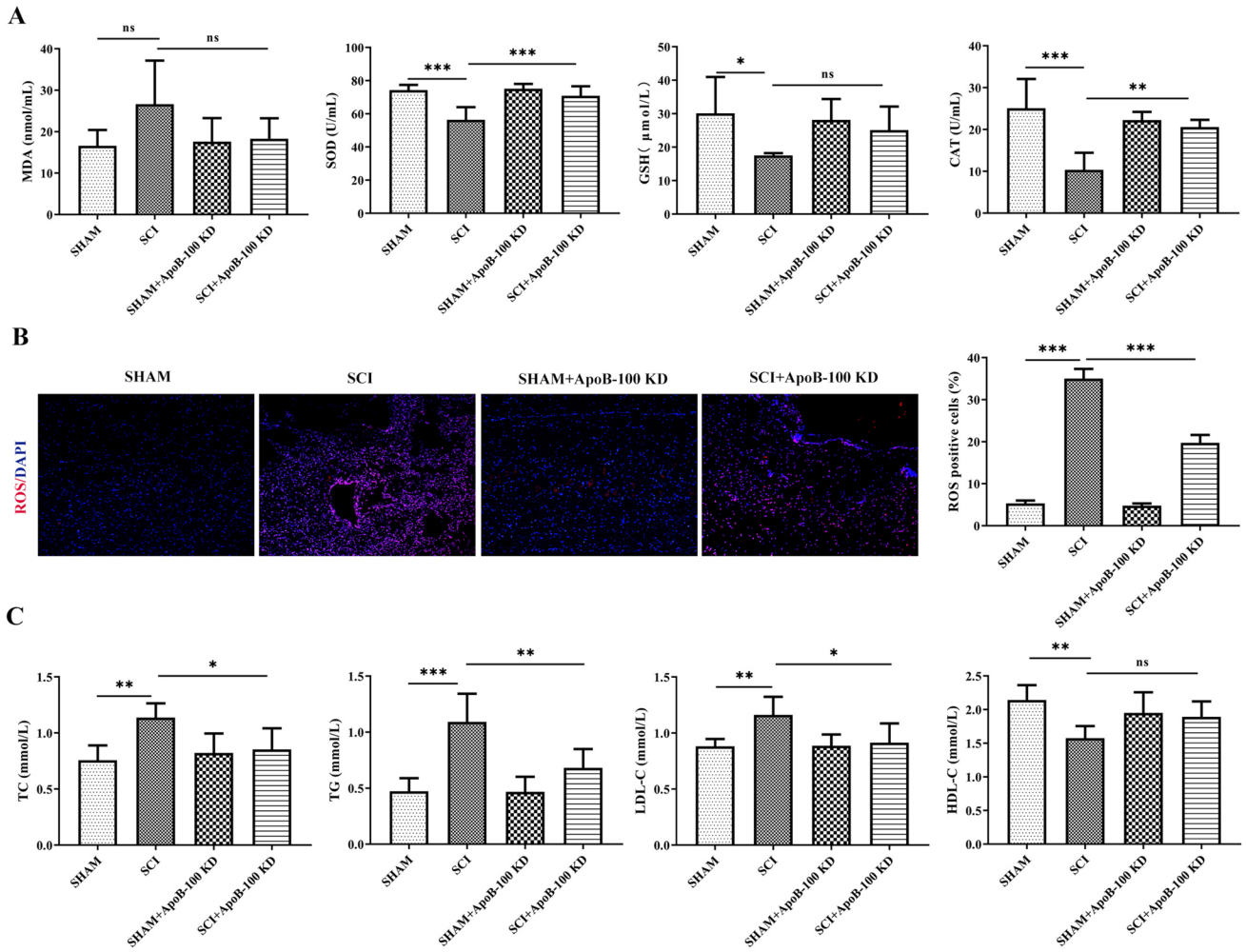

Fig. 4 Knockdown of ApoB-100 inhibits oxidative stress and lipid disorders in SCI mice. **A** The kits were used to measure the levels of oxidative stress–related factors in peripheral blood. **B** Representative images of ROS staining of spinal cord tissues. **C** Biochemical methods were used to detect the levels of lipid factors in peripheral blood samples of mice. *$p < 0.05$, **$p < 0.01$, and ***$p < 0.001$

Knockdown of ApoB-100 Inhibits the Polarization of Macrophages Towards M1 Phenotype

Next, we assessed the impact of ApoB-100 on macrophage polarization of injured spinal cord tissues. As presented in Fig. 5A, compared with the SCI group, the CD86 expression was significantly reduced and iNOS expression was also slightly reduced in the SCI + ApoB-100 KD group, indicating that ApoB-100 knockdown restricted the generation of M1 macrophages of injured spinal cord tissues. However, as shown in Fig. 5B, ApoB-100 knockdown had no significant effect on the expression of CD206 and Arg-1 of injured spinal cord tissues, suggesting that knockdown of ApoB-100 could effectively inhibit the polarization of macrophages to M1 phenotype, but did not affect the polarization of macrophages to M2 phenotype.

Knockdown of ApoB-100 Inhibits Inflammation and Ferroptosis in SCI Mice

TEM was used to observe the changes of the subcellular structure of the injured spinal cord following SCI. The results showed that compared with the SHAM group, cell edema in the SCI group was serious, including cytoplasmic edema, mitochondrial edema, mitochondrial vacuolation, and myelin loss. Compared with the SCI group, mitochondria edema and vacuolation were slightly alleviated in the SCI + ApoB-100 KD group (Fig. 6A). HE staining results showed that compared to the SHAM group, the SCI group had serious spinal nerve tissue lesions with excessive infiltration of inflammatory cells. However, the SCI + ApoB-100 KD group showed moderate nerve tissue lesions, accompanied with some glial cell lesions and necrosis (Fig. 6B). Perls staining results showed obvious iron deposition in the SCI group compared with the

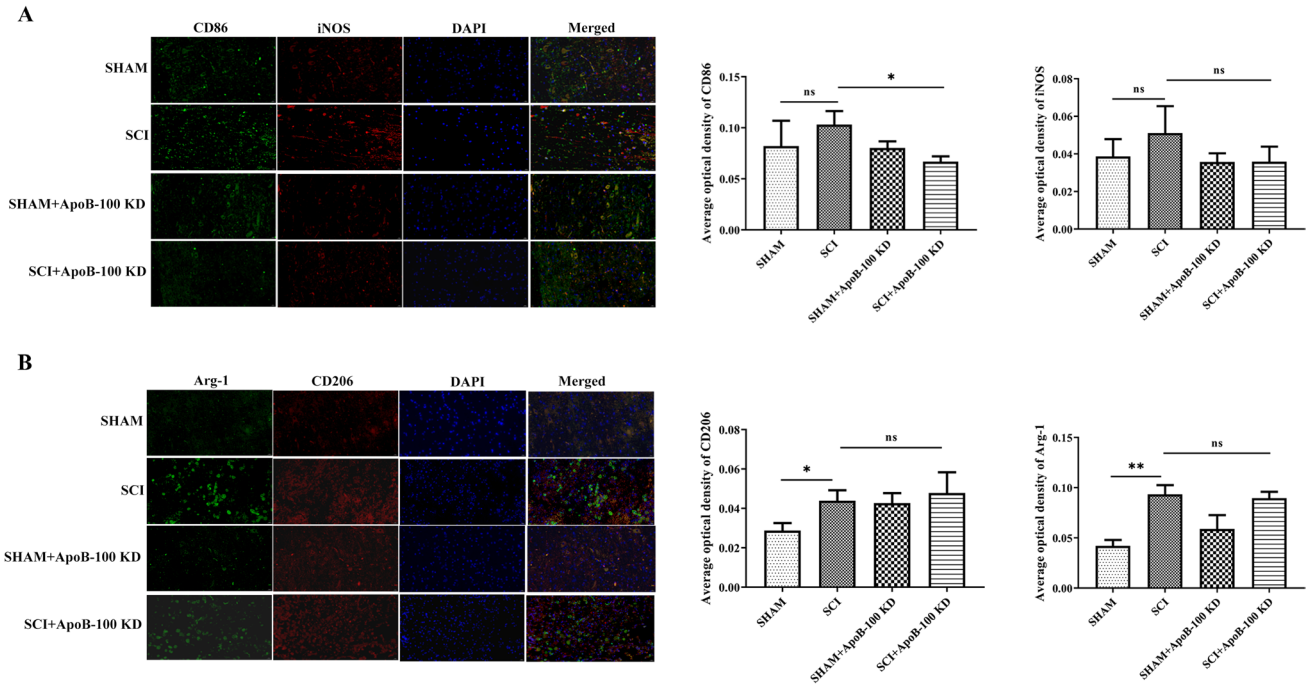

Fig. 5 Knockdown of ApoB-100 inhibits the polarization of macrophages towards M1-type cells. **A** Representative images of immunofluorescence staining of M1 macrophage markers in spinal cord tissues. **B** Representative images of immunofluorescence staining of M2 macrophage markers in spinal cord tissues. $*p < 0.05$, $**p < 0.01$

SHAM group. Compared with the SCI group, it was markedly reduced in the SCI + ApoB-100 KD group (Fig. 6C).

Then, the expression level of proteins related to inflammation/pyroptosis (gasdermin D-N-terminal domain (GSDMD-D), cleaved caspase1 (c-casp1), IL-18, and IL-1β), ferroptosis (transferrin receptor 1 (TFR1), solute carrier family 7a member 11 (SLC7A11), and glutathione peroxidase 4 (GPX4)), lipid metabolism (carnitine O-palmitoyltransferase 1 (CPT1), ApoB-100, and SORT1), and peripheral myelin protein 22 (PMP22) in spinal cord tissues was examined by western blot. The results showed that compared with the SHAM group, the protein expression levels of ApoB-100, IL-1β, IL-18, SORT1, SLC7A11, GSDMD-N, and C-Caspase1 in the SCI group were significantly increased, while the expressions of TFR-1, GPX4, CPT-1, and PMP22 were significantly decreased. Compared with the SCI group, the SCI + ApoB-100 KD group partly reversed above changes (Fig. 6D).

M1 Macrophages Inhibits LPS-Induced ApoB-100/SORT1 Expression, Inflammation, Oxidative Stress, and Ferroptosis in HT22 Neuron Cells, Which Is Further Strengthened by SORT1 Knockdown

Based on above findings, ApoB-100 knockdown could significantly inhibit macrophage polarization towards M1 phenotype following SCI; therefore, RAW264.7 cells were differentiated into M1 phenotype (Fig. 7A), and the conditional medium of M1 macrophages was used to culture HT22 cells to simulate the local immune microenvironment around neurons in vitro. In addition, as aforementioned, SORT1 served as the membrane receptor of ApoB-100, and in vivo experiments above have demonstrated that ApoB-100 knockdown significantly inhibited elevated SORT1 expression following SCI, and thus, whether SORT1 was related to ApoB-100-mediated oxidative stress, inflammation, and ferroptosis deserved to be explored. Hence, as shown in Fig. 7B, compared with the si-NC group, the expression level of SORT1 was significantly reduced after transfection with si-SORT1/2/3. Attributed to a superior transfection efficacy, si-SORT1-2 plasmid was selected for subsequent experiments. Subsequently, HT22 cells were divided into control, LPS, LPS + M1 medium, LPS + M1 medium + si-NC, and LPS + M1 medium + si-SORT1 groups. Compared with the control group, the expression levels of IL-1β, IL-6, and TNF-α were upregulated in the LPS group. Compared with the LPS + M1 medium + si-NC group, interference with SORT1 expression reduced the production of inflammatory cytokines to a certain extent (Fig. 7C). We then measured the expression of adipose-related factors, oxidative stress–related factors, and ApoB-100 at the cellular level, and the results showed that compared with the LPS group, the expression levels of 4-HNE, RBP4, MDA, and ApoB-100 were downregulated in the LPS + M1 medium group, while the expression levels of ADPN, ARG1, SOD, CAT,

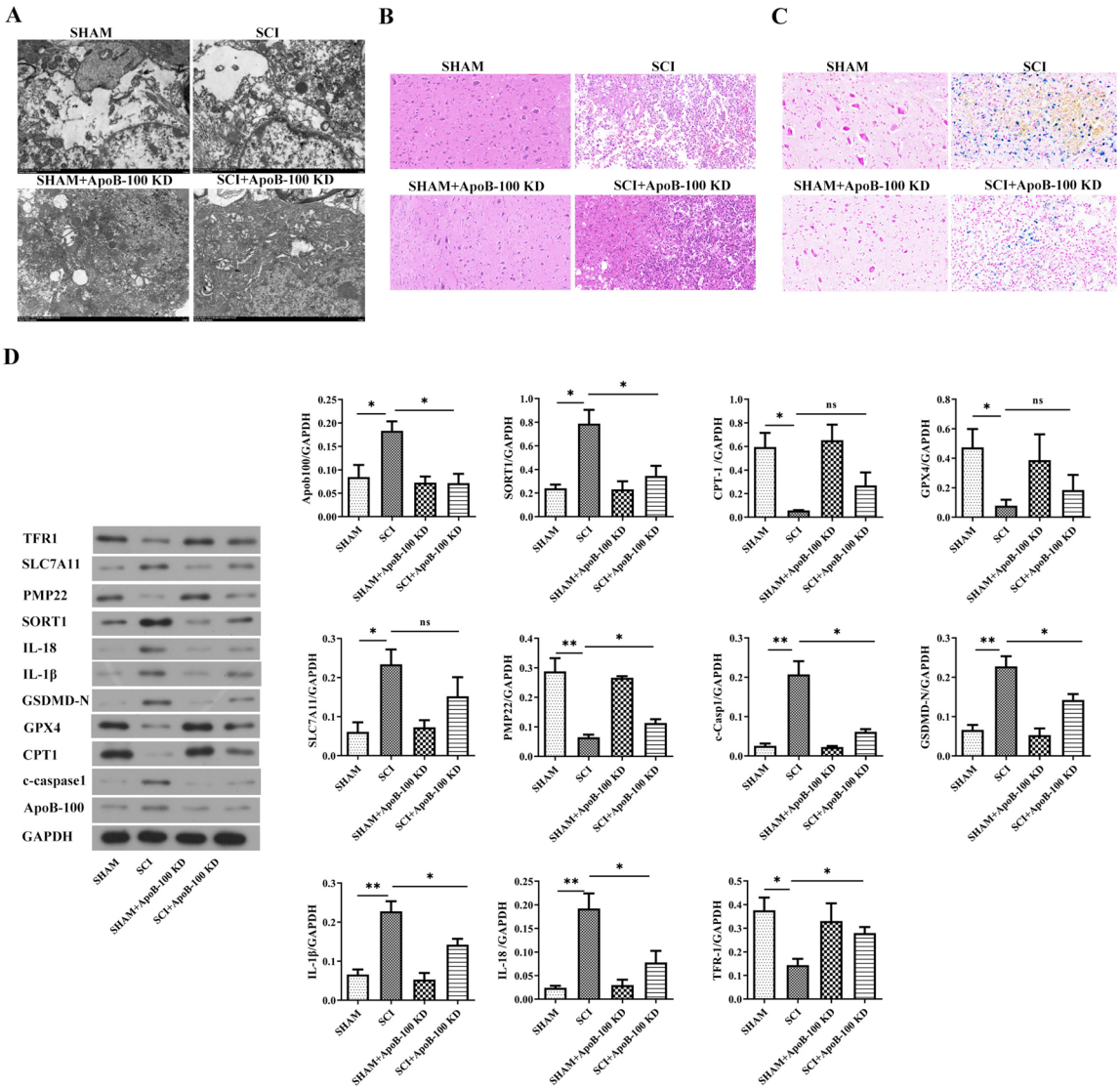

Fig. 6 Knockdown of ApoB-100 inhibits inflammation and ferroptosis in SCI mice. **A** TEM was used to observe the changes of subcellular structure of spinal cord tissues. **B** HE staining was used to detect pathological injury. **C** Perls staining was used to detect iron deposition. **D** The levels of ApoB-100, inflammation-related proteins, and ferroptosis-related proteins in spinal cord tissues were detected by western blot. $^{*}p < 0.05$, $^{**}p < 0.01$

and GSH were upregulated. Compared with the LPS + M1 medium + si-NC group, interference with SORT1 expression downregulated the expressions of 4-HNE, RBP4, ARG1, MDA, and ApoB-100 to some extent, and upregulated the expression levels of ADPN, SOD, CAT, and GSH (Fig. 7D, E).

Finally, the levels of ApoB-100, inflammation-related proteins, and ferroptosis-related proteins in HT22 cells were also detected by western blot. The results showed that, compared with the control group, the protein expression levels of ApoB-100, IL-1β, IL-18, SORT1, SLC7A11, GSDMD-N, and C-Caspase1 were significantly increased in the LPS group, while the expressions of divalent metal transporter 1 (DMT1), TFR-1, GPX4, SLC7A11, and PMP22 were significantly decreased. Compared with the LPS group, the above changes of protein expression were partly inhibited in the LPS + M1 medium group, and the inhibitory effects were further strengthened following SORT1 knockdown to a certain extent (Fig. 8).

Discussion

The spinal cord is mainly composed of mature neurons, which lose the ability to differentiate after differentiation. Once the injury occurs, the spinal cord function

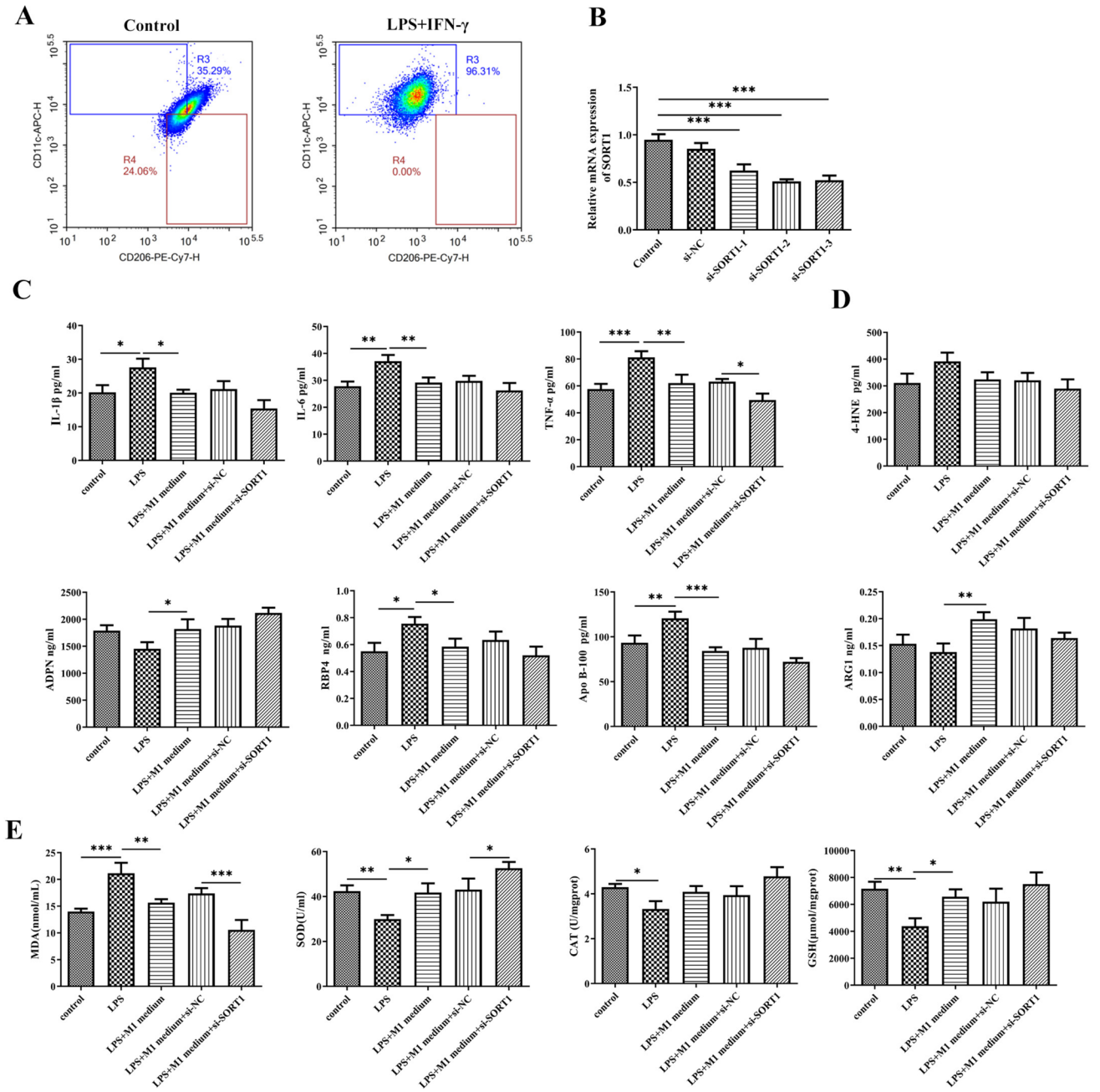

Fig. 7 M1 macrophages inhibit LPS-induced inflammation and oxidative stress in HT22 neuron cells, which is further strengthened by SORT1 knockdown. **A** RAW264.7 cells were induced to differentiate into M1 types, which was verified by flow cytometry. **B** Cell transfection was conducted and transfection efficiency was detected by RT-qPCR. **C** ELISA was used to detect the levels of IL-1β, IL-6, and TNF-α. **D**, **E** The expression of adipose-related factors and oxidative stress–related factors was detected with the kits. $*p<0.05$, $**p<0.01$, and $***p<0.001$

is difficult to rebuild, resulting in a series of disabilities and dysfunction that will affect the lifetime of SCI patients [17]. Therefore, it is the focus of current clinical research to explore the mechanism of SCI and seek regulatory target of SCI. In our article, we constructed the SCI animal model in mice, and the serum TG, TC, LDL, and VLDL-p were detected to be significantly increased, while HDL-c was significantly decreased, indicating the disorder of lipid metabolism in SCI mice. In addition, we also confirmed the occurrence of oxidative stress following SCI. Moreover, the immune microenvironment of SCI mice also changed, accompanied with both elevated M1 and M2 macrophages, and M2 macrophages were dominant.

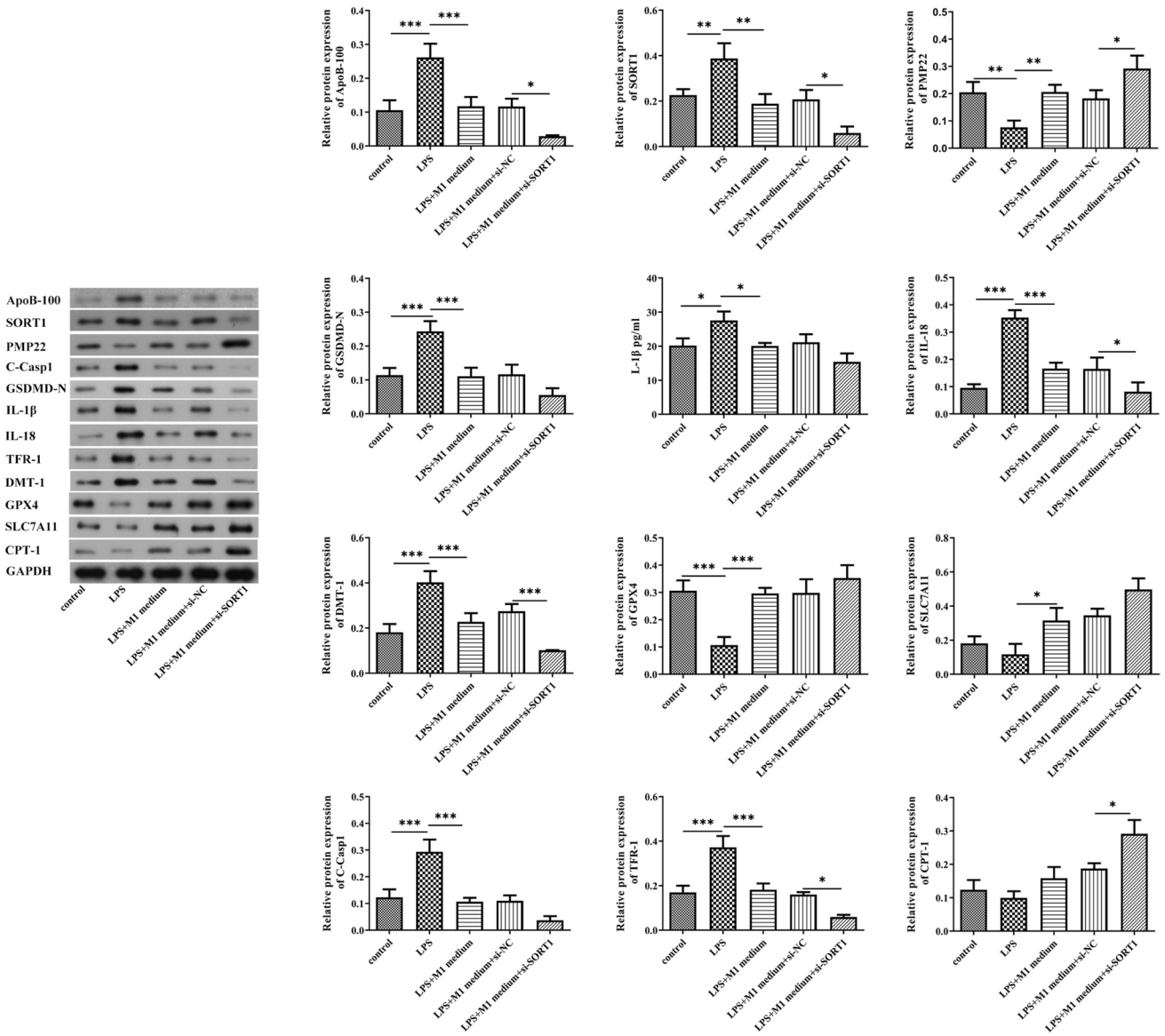

Fig. 8 M1 macrophages inhibit LPS-induced ApoB-100/SORT1 expression, inflammation, and ferroptosis in HT22 neuron cells, which is further strengthened by SORT1 knockdown. The expression levels of ApoB-100/SORT1 expression inflammation-related proteins and ferroptosis-related proteins in HT22 neuron cells were detected by western blot. $^{*}p < 0.05$, $^{**}p < 0.01$, and $^{***}p < 0.001$

As an essential apolipoprotein for the synthesis and secretion of LDL, ApoB100 is a ligand for the endocytosis of LDL particles mediated by low-density lipoprotein receptor (LDLR), and also a major component protein of chylomicron and LDL in plasma [18]. Ox-LDL is a major lipid peroxide, which can induce programmed death of neuronal cells or myelin cells, including ferroptosis, which has been popular in recent years [15]. This programmed death further aggravates the release of inflammatory factors, which seriously affects the balance of M1/M2 macrophage, and significantly damages the structure and function of neuronal cells and their surrounding myelin sheath. Recent study has shown that the expression of ApoB-100 in plasma exosomes in SCI patients is significantly increased [19]. The expression of ApoB-100 protein in SCI patients with severe pressure ulcers was also significantly changed [20]. Consistently, in our experiment, it was found that the expression of ApoB-100 in SCI mice was significantly elevated. Knockout of ApoB-100 could significantly improve functional recovery and relieve oxidative stress, inflammation, lipid disorders, and ferroptosis in injured spinal cord tissues in SCI mice.

So what role does ApoB-100 play in acute SCI? What is the regulatory mechanism? No research has been reported so far. As aforementioned, SORT1 acts as the membrane receptor of ApoB-100, and ApoB-100/SORT1 is critical for the formation of ox-LDL. It has been also reported that SORT1

can restrict the secretion of ApoB-100 under stressed, and SORT1 mutation in diabetes is associated with a decrease of plasma ApoB, TG, and LDL [21]. This may be one of the important ways that ApoB-100 is involved in ox-LDL-related SCI. In the present study, in vivo experiments demonstrated that ApoB-100 knockdown not only significantly inhibited the elevated LDL level following SCI, but also inhibited SORT1 expression, and thus, we speculated that SORT1 might be related to ApoB-100-mediated macrophage polarization, oxidative stress, inflammation, and ferroptosis during the development of SCI. Therefore, in cell experiments, as ApoB-100 knockdown might attenuate SCI partly through inhibiting M1 macrophages, conditional medium from M1 macrophages was used to culture HT22 cells to mimic the local immune microenvironment around neurons in vitro. The results showed that LPS caused increased expression of ApoB-100 in neuron cells, and SORT1 knockdown in HT22 cells inhibited ApoB-100 and also attenuated LPS-induced inflammation, oxidative stress, lipid peroxidation, and ferroptosis in neurons.

And last but not least, we found that the conditional medium from M1-type macrophage in vitro significantly inhibited the inflammatory response, oxidative stress, and ferroptosis levels of injured neuronal cells, which was inconsistent with the results in vivo. Some researchers believe that within 7 days after SCI, macrophages and microglia are mixed with M1 type and M2 type, and M1 type still plays a positive role during this time, but with the passage of time, the proportion of M2 type gradually decreases to disappear, while M1 type gradually increases and dominates for a long time, which may be the main reason for the unsatisfactory recovery in chronic phase [22]. In addition, M2-type macrophages/microglia mainly secrete TGF-β, Arg-1, and type I and type III collagen, which are indeed beneficial to inflammation inhibition and tissue repair, while they promote the formation of glial scar in astrocytes, which is considered to be an adverse factor to the electrical conduction function of neurons [23]. M1-type macrophage plays an important role in clearing bacterial infection and activating adaptive immunity to produce antigen presentation, as well as activating the antioxidant system, which is conducive to the recovery of SCI in the acute phase [9]. The above studies and our experimental results suggest that the M1-type macrophage microenvironment itself may be beneficial at a certain stage during SCI, but our in vivo results show that the M1-type macrophage microenvironment promotes the occurrence of SCI diseases, which is harmful. One possible reason is that M1-type macrophages are over-induced in SCI mice, which triggers the inflammatory cascade reaction and eventually leads to the undesirable result of deteriorating SCI disease symptoms. Secondly, although ApoB-100 knockdown in SCI mice inhibits the polarization to M1-type macrophages but does not affect M2-type macrophages, the ratio of M1/M2 macrophages is thus changed, which may partly restore the immune microenvironment to attenuate inflammation and oxidative stress following SCI.

Anyway, there were still several limitations in this study. Firstly, we only investigated the regulatory role of ApoB-100 at 7th day following SCI; however, in the acute period of SCI, the changes of macrophages/microglia were complicated, and more time points to record these changes may enrich the data about immune microenvironment following SCI. Secondly, more solid data, rather than the bar graph, will be beneficial to further verify the conclusions. Finally, further regulatory mechanism underlying ApoB-100/SORT1 to affect SCI progression needs to be discovered in our future work.

Conclusion

In conclusion, ApoB-100 is a critical pathogenic factor contributing to the development of SCI. Blockage of ApoB-100/SORT1-mediated immune microenvironment plays a protective role against SCI via inhibiting oxidative stress, inflammation, lipid disorders, and ferroptosis, providing novel insights of the targeted therapy of SCI.

Author Contribution GX and ZC designed the experiments; CW, CJ, DQ, CL, JC, JZ, and GB conducted the experiments; CW, CJ, DQ, and CL analyzed and interpreted the data; CW and CJ drafted the manuscript; GX and ZC revised the manuscript. All authors have read and approved the final manuscript.

Funding This work was supported by the National Natural Science Foundation of China (82202436), Science and Technology Projects in Jiangsu Province (BE2023742), Medical Research Project of Jiangsu Provincial Health Commission (ZDB2020004), Research Project of Nantong Health Commission (MA2021016, MS2022016), Nantong Science and Technology Project (MS22022004, JC22022067), and High-level Science and Technology Project Nurturing Fund of Nantong First People's Hospital (YPYJJZD009).

Data Availability All data have been included in this article.

Declarations

Ethics Approval All animal studies were conformed to ethical standards and approved by the ethic committee of Nantong First People's Hospital.

Consent to Participate Not applicable.

Consent for Publication Not applicable.

Competing Interests The authors declare no competing interests.

References

1. Michinaga S, Koyama Y (2021) Pathophysiological responses and roles of astrocytes in traumatic brain injury. Int J Mol Sci 22(12):6418
2. Xu L et al (2021) T-cell infiltration, contribution and regulation in the central nervous system post-traumatic injury. Cell Prolif 54(8):e13092
3. Quadri SA et al (2020) Recent update on basic mechanisms of spinal cord injury. Neurosurg Rev 43(2):425–441
4. Katoh H, Yokota K, Fehlings MG (2019) Regeneration of spinal cord connectivity through stem cell transplantation and biomaterial scaffolds. Front Cell Neurosci 13:248
5. Golestani A et al (2022) Epidemiology of traumatic spinal cord injury in developing countries from 2009 to 2020: a systematic review and meta-analysis. Neuroepidemiology 56(4):219–239
6. Courtine G, Sofroniew MV (2019) Spinal cord repair: advances in biology and technology. Nat Med 25(6):898–908
7. Tran AP, Warren PM, Silver J (2018) The biology of regeneration failure and success after spinal cord injury. Physiol Rev 98(2):881–917
8. Lech M, Anders HJ (2013) Macrophages and fibrosis: how resident and infiltrating mononuclear phagocytes orchestrate all phases of tissue injury and repair. Biochim Biophys Acta 1832(7):989–997
9. David S, Kroner A (2011) Repertoire of microglial and macrophage responses after spinal cord injury. Nat Rev Neurosci 12(7):388–399
10. Paim LR et al (2013) Oxidized low-density lipoprotein, matrix-metalloproteinase-8 and carotid atherosclerosis in spinal cord injured subjects. Atherosclerosis 231(2):341–345
11. Paim LR et al (2019) Circulating microRNAs, vascular risk, and physical activity in spinal cord-injured subjects. J Neurotrauma 36(6):845–852
12. Morita SY (2016) Metabolism and modification of apolipoprotein B-containing lipoproteins involved in dyslipidemia and atherosclerosis. Biol Pharm Bull 39(1):1–24
13 Kjolby M et al (2010) Sort1, encoded by the cardiovascular risk locus 1p13.3, is a regulator of hepatic lipoprotein export. Cell Metab 12(3):213–23
14. Zhang B et al (2020) Lipid accumulation and injury in primary calf hepatocytes challenged with different long-chain fatty acids. Front Vet Sci 7:547047
15. Su G et al (2021) SIRT1-autophagy axis inhibits excess iron-induced ferroptosis of foam cells and subsequently increases IL-1Beta and IL-18. Biochem Biophys Res Commun 561:33–39
16. He Z et al (2017) Inhibition of endoplasmic reticulum stress preserves the integrity of blood-spinal cord barrier in diabetic rats subjected to spinal cord injury. Sci Rep 7(1):7661
17. Anjum A et al (2020) Spinal cord injury: pathophysiology, multimolecular interactions, and underlying recovery mechanisms. Int J Mol Sci 21(20):7533
18. Brodsky JL, Fisher EA (2008) The many intersecting pathways underlying apolipoprotein B secretion and degradation. Trends Endocrinol Metab 19(7):254–259
19. Wu C et al (2021) Bioinformatic analysis of the proteome in exosomes derived from plasma: exosomes involved in cholesterol metabolism process of patients with spinal cord injury in the acute phase. Front Neuroinform 15:662967
20. Baldan-Martin M et al (2020) Comprehensive proteomic profiling of pressure ulcers in patients with spinal cord injury identifies a specific protein pattern of pathology. Adv Wound Care 9(5):277–294 (**New Rochelle**)
21. Conlon DM et al (2022) Sortilin restricts secretion of apolipoprotein B-100 by hepatocytes under stressed but not basal conditions. J Clin Invest 132(6):e144334
22. Kigerl KA et al (2009) Identification of two distinct macrophage subsets with divergent effects causing either neurotoxicity or regeneration in the injured mouse spinal cord. J Neurosci 29(43):13435–13444
23. Karimi-Abdolrezaee S, Billakanti R (2012) Reactive astrogliosis after spinal cord injury-beneficial and detrimental effects. Mol Neurobiol 46(2):251–264